Implementation of an EDMF boundary-layer and shallow-cumulus parameterization into SAM

Wolfgang Langhans

August 3, 2016

Contents

1 Introduction

For any prognostic variable ψ we seek to represent its tendency due to unresolved turbulent transport. Thereby, ψ is one of u, v, h_{li}, q_t, q_p, and e (i.e., TKE). Here, mixing ratio q_t is defined as the mass of water vapor and cloud condensate (liquid and frozen) per mass of dry air, as $q_t = q_v + q_n = q_v + q_c + q_i$. The mixing ratio for precipitating water is the sum of mixing ratios for rain, snow, and graupel, $q_p = q_r + q_s + q_g$. It is common in GCMs and mesoscale models to assume that the vertical velocity w has no tendency from subgrid-scale transport. On top of that, subgrid transport is assumed to be vertical only.

The tendency for any variable ψ is then obtained from the EDMF equation as

$$\left(\frac{\partial \psi}{\partial t}\right)_{turb} = -\frac{1}{\overline{\rho}}\frac{\partial}{\partial z}\overline{\rho}\left(ED^{\psi} + MF^{\psi}\right) = -\frac{1}{\overline{\rho}}\frac{\partial}{\partial z}\overline{\rho}\left(-K_{\psi}(z)\frac{\partial \psi(z)}{\partial z} + \sum_i M_i(z)(\psi_i^{up}(z) - \psi(z))\right) \quad (1)$$

with $\overline{\rho}$ the horizontally averaged density of dry air. Here, ED is the eddy-diffusivity part and MF the (multiplume) mass-flux part of the turbulent flux. Closure is provided by specifying K_ψ, M_i, and ψ_i^{up} for each updraft i.

The necessary/provided input to the EDMF parameterization is listed in section 2. The closure is described in section 3. The implicit numerical procedure to solve Eq. (1) is outlined in section 4. One key advantage of this multiplume EDMF parameterization is that PBL mixing and shallow cumulus cloud cover are parameterized in a unified way since plumes might eventually get saturated. For this reason, subgrid-scale cloud cover from shallow cumulus is also provided from the multiplume model. A large-scale saturation scheme based on a subgrid-scale PDF scheme is also implemented to represent effects of stratocumulus clouds (see section ??).

2 Input

2.1 From SAM

In this 1D framework let index k represent the vertical center of cell k. Let indices $k-1/2$ and $k+1/2$ indicate the position of the bottom and top interface of cell k. Thus, the input is u^k, v^k, w^k, h_{li}^k, q_v^k, and e^k with k ranging from 1 to the total number of cells N_k in the 1D column. On top of that, $\overline{\rho}^k$ and $\overline{\rho}^{k\pm1/2}$ will be needed.

Also needed for the parameterization of eddy diffusivities is the squared characteristic rate of strain $\overline{D}^2$ (based on grid-scale velocities) as defined in Eq. (12) at cell centers. Note that SAM uses an Arakawa-C grid but let's for ease of documentation assume that all variables are located at cell centers.

2.2 From surface flux parameterization

The parameterization of surface fluxes over ocean surface is based on Bryan et al. (2003) and has been used also in SAM (Khairoutdinov and Randall, 2003) and CAM (see Collins et al., 2004, section 4.10.2). A formulation for fluxes over land is also available but not yet included. The formulation is adapted here to our needs as explained below. A bulk drag/transfer law is used for the surface turbulent fluxes of u, v, θ, and q_v, given as

$$(\tau, E, H) = -\rho_1 |\mathbf{v_{h1}}| (C_d \mathbf{v_{h1}}, C_e \Delta q_v, C_\theta \Delta\theta) \tag{2}$$

with $\Delta q_v = q_{v1} - q_v^*(T_s)$, $\Delta\theta = \theta_1 - \theta_s$, $\mathbf{v_h}$ the horizontal wind vector, and C_d, C_e, and C_θ the transfer coefficients for momentum, q_v, and θ. T_s is the surface temperature and $q_v^*(T_s)$ the saturation mixing ratio at the surface temperature. Index "1" indicates values on the first model level.

Turbulent velocity scales u_*, q_{v*}, and θ_* are introduced in the formulation of these fluxes as

$$\begin{aligned} u_* &= (\overline{u'w'}^2 + \overline{v'w'}^2)^{1/4} = C_d^{1/2} |\mathbf{v_{h1}}| && (3) \\ q_{v*} &= -\overline{q_v' w'}/u_* = C_e |\mathbf{v_{h1}}| \Delta q_v / u_* && (4) \end{aligned}$$

The parameterization characterizes the surface layer stability based on the Monin-Obukhov length and then distinguishes between flux profiles for stable and unstable conditions. The parameterization proceeds by utilizing similarity theory to determine the drag coefficients C_d, C_e, and C_θ and the respective fluxes. That is, the parameterization provides the momentum and sensible and latent heat fluxes. The required flux of h_{il} in kinematic units is obtained as

$$\overline{h_{il}' w'} = c_p H. \tag{5}$$

3 EDMF closure

The task of the parameterization is to provide the eddy diffusivities K_ψ and M_i and ψ_i^{up} for each updraft i. A variety of flavors of a 1.5 TKE closure are implemented and described below. The updraft properties are obtained through a multiplume model that was kindly provided by Kay Suselj/JPL and is somewhat modified here.

3.1 Eddy-diffusivity models

The eddy diffusivities are computed at cell centers and averaging provides $K_\psi^{k\pm1/2}$ at cell interfaces.

3.1.1 Teixeira TKE closure

The formulation of the TKE boundary layer scheme follows the description given by Teixeira and Cheinet (2004) and is specifically designed here to model the evolution of the dry convective boundary layer. The prognostic equation for e, the sgs kinetic energy per unit dry air, is

$$\frac{\partial e}{\partial t} = \mathrm{ADV} + \mathrm{TRANS} + \mathrm{SHEAR} + \mathrm{BUOY} - \mathrm{DISS} \tag{6}$$

and in this parameterization the individual sources/sinks are closed as

$$\mathrm{TRANS} = \frac{1}{\overline{\rho}}\frac{\partial}{\partial z}(\overline{\rho_d} K_m \frac{\partial e}{\partial z}) \tag{7}$$

$$\mathrm{SHEAR} = K_m \overline{D}^2 \tag{8}$$

$$\mathrm{BUOY} = \frac{g}{\theta_v}\overline{w'\theta_v'} \tag{9}$$

$$\mathrm{DISS} = c_\epsilon \sqrt{e}/l_\epsilon \tag{10}$$

with $K_m = c_k l e^{1/2}$, $l_\epsilon = l/2.5$, $c_\epsilon = 0.16$, and $c_k = 0.5$. The buoyancy flux $\overline{w'\theta_v'}$ is generally taken to be the ED part (even if a MF part exists).

The square of the characteristic rate of strain $\overline{D}^2$ is generally defined as $\overline{D}^2 = 2D_{ij}D_{ij}$ with element (i, j) of the tensor given as

$$D_{ij} = \frac{1}{2}(\frac{\partial u_i}{\partial x_j} + \frac{\partial u_j}{\partial x_i}) \tag{11}$$

with capital u_i indicating the grid-scale velocity in direction i of the cartesian coordinate system. After summation one obtains

$$\overline{D}^2 = 2\{D_{11}^2 + D_{22}^2 + D_{33}^2\} + 4\{D_{12}^2 + D_{13}^2 + D_{23}^2\}. \tag{12}$$

In the here relevant 1D case this reduces to $\overline{D}^2 = (du/dz)^2 + (dv/dz)^2$.

The eddy diffusivity for heat and moisture is $K_h = \mathrm{Pr}K_m$ with $\mathrm{Pr} = 1$. The mixing length is obtained as

$$l = \tau\sqrt{e} + (\kappa z - \tau\sqrt{e})e^{-z/\alpha} \tag{13}$$

with $\alpha = 100$ m and τ taken to be either 600 sec or $\tau = 0.5h/w^*$ with $w^* = (hg/\theta_{v0}\overline{w'\theta_v'}|_0)^{1/3}$.

The boundary layer height h is defined as either the height where the buoyancy flux from the previous step is minimized (a somewhat inconsistent numerical treatment) or as the height where the θ_v gradient at step n is maximized. A third option to obtain h is made available through code adapted from WRF and implies an evaluation of both e and θ_v profiles.

3.1.2 Witek TKE closure

The Witek closure follows mostly the description given by Witek et al. (2011). However, it is an EDMF closure. The MF model is described below. The ED part is very similar to the above described Teixeira closure. Only the differences are described here.

The MF part of the buoyancy flux is considered in the buoyancy production term for TKE. This is argued to produce a proper buoyancy profile near the slightly stable parts of the BL and at the inversion. Moreover, some constants and the disspiation length take different values/definitions:

$$c_k = 0.425 \tag{14}$$

$$Pr = 0.5882 \tag{15}$$

$$C_\epsilon = 0.304 \tag{16}$$

$$l_\epsilon = l \tag{17}$$

The definition of the length scale differs from Witek's paper and is closer to the proposal be Sušelj et al. (2013):

$$
\begin{aligned}
l &= l_{23} + (\kappa z - l_{23}) e^{-z/\alpha} && (18)\\
l_{23}^{-1} &= l_2^{-1} + l_3^{-1} && (19)\\
l_2 &= \tau \sqrt{e} && (20)\\
l_3 &= \begin{cases} \max(\Delta z/2, 0.7\sqrt{(e/N^2)}) & \text{if} \quad N^2 > 0 \\ \infty & \text{if} \quad N^2 \le 0. \end{cases} && (21)
\end{aligned}
$$

In neutral or unstable conditions it is the same as for the Teixeira closure as long as α and τ receive the same definitions (i.e., $\alpha = 100$ m and $\tau = 0.5h/w_*$). However, in locally stable conditions the length scale gets reduced. Here, τ may take a constant value of 400 s (same as in Sušelj et al. (2013)) or be defined as in the Teixeira closure as $\tau = 0.5h/w_*$. We avoid the exact definition from Witek et al. (2011) since it would require the computation of the friction velocity u_* based on surface layer similarity theory. It is more complicated to define the latter under calm conditions and thus avoided so far.

3.1.3 Emerging reference TKE closure

Goal: Add description of emerging TKE closure that will be used in the Dycore. The keys to a successful (i.e., applicability in different PBLs, possibility to MF extension) TKE closure should be highlighted and reviewed.

3.2 Multiplume model

3.2.1 Description

The multiplume model provides updraft properties for a user-specified number of non-precipitating entraining plumes and thus the MF part in Eq. (1). It closely follows the proposed multiplume model of Cheinet (2003) but is formulated more generally to account for other existing formulations. Each plume represents one class of updrafts with the same initial thermodynamic and kinematic properties. Note that in Eq. (1) it has been assumed that ψ of the undisturbed subsiding air in the environment equals the grid-box mean ψ. This is equivalent to assuming that the updraft/downdraft area is small. This assumption is not made in, e.g., Cheinet (2003), but we stick to this for now. Following Sušelj et al. (2012), Sušelj et al. (2013), and Sušelj et al. (2014) the MF part is assumed to be zero in case of ψ equal to u, v, or e (Can we add these MF tendencies for u, v, or e?). This is generally justified by the smaller eddy viscosities for momentum than for heat and the general lack in knowledge about sources/sinks of momentum within a rising plume (see, e.g., discussion in Han, 2015). Index i identifies an individual updraft class among a total of N^{up} (to be specified, e.g., $N^{up} = 10$) updrafts. M_i is defined as $s_i w_i^{up}$ with s_i and w_i^{up} the fractional weight and vertical velocity, respectively, of updraft class i.

Initial conditions are obtained as in Cheinet (2003) and Lenschow et al. (1980). Through similarity theory the initial conditions are linked to surface fluxes, boundary layer depth, and an assumed PDF of the vertical velocity. The latter is assumed to be a Gaussian with a standard deviation σ_w, given as

$$
f_w(w) = \frac{1}{\sigma_w 2\pi} e^{-\frac{w^2}{2\sigma_w^2}}. \tag{22}
$$

A fixed number of plume classes spans a discrete PDF for a selected range between $w_{\min}$ and $w_{\max}$. Thereby, $w_{\min}$ is typically thought to be larger than zero since weak eddies are accounted for by the ED part. Class i covers all plumes with vertical velocities between

$$
\begin{aligned}
w_i^{\min} &= w_{\min} + (i-1)(w_{\max} - w_{\min})/N^{up} \qquad \text{and} && (23)\\
w_i^{\max} &= w_{\min} + i(w_{\max} - w_{\min})/N^{up}, && (24)
\end{aligned}
$$

has a fractional weight

$$
s_i = \int_{w_i^{\min}}^{w_i^{\max}} dw \; f_w(w) = 1/2(\mathrm{erf}(\frac{w_i^{\max}}{\sqrt{2}\sigma_w}) - \mathrm{erf}(\frac{w_i^{\min}}{\sqrt{2}\sigma_w})), \tag{25}
$$

and an average initial updraft velocity

$$w_i = 1/s_i \int_{w_i^{\min}}^{w_i^{\max}} dw\ f(w)\ w = \frac{\sigma_w}{s_i\sqrt{2\pi}}(e^{-\frac{w_i^{\min 2}}{2\sigma_w^2}} - e^{-\frac{w_i^{\max 2}}{2\sigma_w^2}}). \tag{26}$$

This initial average velocity has been modified here from the original $1/2(w_i^{\min} + w_i^{\max})$ used by Kay/JPL in order to make sure that the total upward mass flux $\int_0^\infty dw\ f_w w = \sum_{i=1,N_p} s_i w_i$ is independent of N_p. To illustrate the difference, if $w_{\min} = 0$ and $w_{\max} \gg \sqrt{2}\sigma_w$ then the total area covered by the discretized updraft class spectrum is $A_tot = 0.5$. Then, if only one plume was used the average initial velocity obtains the correct mean value $w_1 = \sqrt{\frac{2}{\pi}}\sigma_w$. In contrast, the unmodified code gives $0.5w_i^{\max}$ (which would be correct only if $w_i^{\max} = 2\sqrt{2/\pi\sigma_w}$). This update should allow for better convergence characteristics with an increasing number of plumes.

The actual physical area a_i of one plume within a class spanned between $w_i^{\min}$ and $w_i^{\max}$ results from

$$A_i/A_{tot} = s_i = \int_i dw\ f(w) = 1/A_{tot}\int_i dw\ N(w)a(w) \tag{27}$$

with $N(w)$ the number density $[(\mathrm{m\ s^{-1}})^{-1}]$ of plumes as a function of velocity and $a(w)$ the plume area size as function of vertical velocity. If we assume that each class has a mean number and mean size of plumes then we can rewrite this, as $s_i = a_i/A_{tot}N_i$, such that

$$a_i = s_i A_{tot}/N_i. \tag{28}$$

Thus, specifying N_i in addition is necessary in order to specify the size of plumes and thus their mass flux and eventually entrainment rates. The same weighting factor s_i might correspond to a large number of plumes with small fractional area or to a small number of plumes with large fractional area. The outcome might be largely different. Let's discuss this.

To obtain initial conditions, we follow Lenschow et al. (1980) and diagnose the standard deviations of w, θ, and q_v from the surface layer similarty relations

$$\sigma_w = 1.34w^*(z_s/h)^{1/3}(1-0.8z_s/h) \tag{29}$$
$$\sigma_{q_t} = 1.34q_v^*(z_s/h)^{-1/3} \tag{30}$$
$$\sigma_\theta = 1.34\theta^*(z_s/h)^{-1/3} \tag{31}$$

with

$$w^* = (hg/\theta_v \overline{w'\theta_v'})^{1/3} \tag{32}$$
$$q_v^* = \overline{w'q_v'}/w^* \tag{33}$$
$$\theta^* = \overline{w'\theta'}/w^* \tag{34}$$
$$\tag{35}$$

and z_s is set to be 50 meter and supposed to be in the surface layer. As shown by (Sorbjan, 1991, see their Fig. 12), the correlation coefficient between water vapor and potential temperature is $r_{q_v\theta} \approx 0.75$ (note that Cheinet (2003) gets this number wrong) in the surface layer such that the standard deviation of virtual potential temperature can be obtained, as

$$\sigma_{\theta_v} = (\sigma_\theta^2 + 0.61^2\theta^2\sigma_{q_t}^2 + 2\cdot 0.61\theta r_{q_v\theta}\sigma_\theta\sigma_{q_t})^{1/2}. \tag{36}$$

The correlation coefficient $r_{q_v\theta}$ might be different over a water surface, right? (even negative: cold pools picking up vapor from ocean)

Finally, the perturbations to the mean values are obtained – again using correlation coefficients from Cheinet (2003) – as

$$q_{ti} = q_v + 0.32w_i\sigma_{q_t}/\sigma_w \tag{37}$$
$$\theta_{vi} = \theta_v + 0.58w_i\sigma_{\theta_v}/\sigma_w \tag{38}$$
$$h_{li} = c_p\frac{T}{\theta}\theta_{vi}/(1+\epsilon q_{vi}) \quad \text{since } q_{ci} = q_{ii} = 0. \tag{39}$$

If we decide to use a single plume model ($N^{up} = 1$), then we might alternatively opt for the initial conditions defined in Soares et al. (2004) and Witek et al. (2011). Therein,

$$\theta_{v1} = \theta_v + \beta\overline{\theta_v' w'}/e^{1/2} \tag{40}$$

with β typically set to 0.3 (Soares et al., 2004; Witek et al., 2011). An analogous relation is used to relate q_v to the surface latent heat flux. The intial vertical velocity is zero. Note that β will set the intial plume buoyancy. The fractional area of the plume is assumed to be $s_i = 0.1$.

Steady-state entraining plumes are then used to describe the vertical thermodynamic and dynamic profiles. A conserved quantity ψ follows the vertical profile given by

$$\frac{d\psi_i^{up}}{dz} = -\epsilon(\psi_i^{up} - \psi) \tag{41}$$

with entrainment rate ϵ and the environmental value ψ. The parcel rises until its vertical velocity reaches zero. The latter is given by Simpson and Wiggert (1969)'s parameterization

$$1/2\frac{d(w_i^{up})^2}{dz} = aB_i^{up} - (b + c\epsilon)(w_i^{up})^2 \tag{42}$$

with buoyancy $B_i^{up} = g(\theta_v^{up}/\theta_v - 1)$, the environmental profile θ_v, and constants $a = 2/3$, $b = 0.002\ \mathrm{m}^{-1}$, $c = 1.5$. The three acceleration terms are buoyancy, form drag, and mixing drag.

Entrainment is described by either a Poisson process (see next section), by a fixed fractional entrainment rate $\epsilon = \epsilon 0$, by Witek et al. (2011)'s formulation

$$\epsilon = \frac{0.7}{l} \tag{43}$$

or by Neggers et al. (2002)'s formulation

$$\epsilon = \frac{\alpha_n}{\tau w} \tag{44}$$

with $\tau = h/w_*$ the eddy turnover time as defined before and α_n a tuning parameter.

The conserved variables used in the plume equations are liquid/frozen moist static energy h_{li} and total water mixing ratio $q_t = q_v + q_n$. Equation (49) is solved for these two variables until the vertical velocity in a plume turns zero. At each height a saturation adjustment scheme is used to infer the condensed water content q_c and q_i, q_v, and θ_v.

3.2.2 Emerging reference MF closure

Goal: Add description of emerging MF closure that will be used in the Dycore. The keys to a successful (i.e., applicability in different PBLs, skill in representing cloud cover, match with ED closure) MF closure should be highlighted and reviewed.

3.2.3 Discretization

Solving the vertical velocity and scalar equation in the vertical is accomplished as in Šuselj et al. (2014) (see their appendix). Thereby we assume that ϵ, the environment value ψ, and buoyancy B can be considered constant in each layer (instead of, e.g., $\epsilon(\psi^{up} - \psi)$ being constant) to obtain an analytical expression for ψ at the next level. This method has the numerical advantage that ψ^{up} at the next higher level will be bound in between the value of ψ^{up} at the lower level and the environmental value of ψ in that layer. This provides the mass flux properties ($M_i^{k\pm1/2}$ and $\psi_i^{up\ k\pm1/2}$) on cell interfaces. The discretized equations are

$$\psi_i^{up\ k+1/2} = \psi^{\ k}(1 - e^{-\epsilon^k \Delta z^k}) + \psi_i^{up\ k-1/2} e^{-\epsilon^k \Delta z^k} \tag{45}$$

$$(w_i^{up\ k+1/2})^2 = (\alpha w_i^{up\ k-1/2})^2 + (1 - \alpha^2)\frac{aB_i^{up\ k}}{b + c\epsilon^k}, \tag{46}$$

where $\alpha = e^{-(b+c\epsilon^k)\Delta z^k}$ and $B_i^{up\ k} = g(0.5(\theta_{vi}^{up\ k+1/2} + \theta_{vi}^{up\ k-1/2})/\theta_v^k - 1)$. IF a stochastic formulation is used then the entrainment rate (m^{-1}) in layer Δz^k is computed as

$$\epsilon(\Delta z^k) = \frac{1}{\Delta z^k}\epsilon_d \mathcal{P}(\frac{\Delta z^k}{L_0}) \tag{47}$$

with $\epsilon_d = 0.1$, $L_0 = 100$ m, and $\mathcal{P}$ a random number drawn from the Poisson distribution; otherwise, one of the above mentioned deterministic formulations is used.

4 Solving for the tendencies

4.1 EDMF equation

Equation (1) needs to be solved to obtain the tentendy from mixing. The spatial discretization of the equations is done using a centered scheme for the diffusion term and the mass-flux term. K, M_i, and ψ_i^{up} are treated explicitly in time while other terms can be implicit. For brevity we drop index $_\psi$ here for eddy diffusivities K. The vertical grid structure and the indexing is illustrated in Fig. 1 and is the same as used by Tiedtke (1989). An important stability criterion – realized by Tiedtke (1989) – is that the environmental value of ψ at the interface $k+1/2$ can not be taken as the average between k and $k+1$. The interface value of ψ is needed in the subsidence term $-\psi(z)\sum_i M_i(z)$ and in line with an upwind discretization has to be interpolated/taken from above. We simply assume $\psi^{k+1/2} = \psi^{k+1}$ and $\psi^{k-1/2} = \psi^k$. We find that taking the average indeed results in numerical instabilities, while this approach works fine. The discretized form of Eq. (1) is then

$$
\begin{aligned}
&\frac{\psi^{n+1,k} - \psi^{n,k}}{\Delta t} = \\
&-\frac{1}{\rho^{n,k}\Delta z^k}\left\{-\frac{K^{n,k+1/2}\rho^{n,k+1/2}}{\Delta z^{k+1/2}}[\beta_1^+(\psi^{n+1,k+1} - \psi^{n+1,k}) + \beta_1^-(\psi^{n,k+1} - \psi^{n,k})]\right. \\
&+\frac{K^{n,k-1/2}\rho^{n,k-1/2}}{\Delta z^{k-1/2}}[\beta_1^+(\psi^{n+1,k} - \psi^{n+1,k-1}) + \beta_1^-(\psi^{n,k} - \psi^{n,k-1})] \\
&+\rho^{n,k+1/2}\left[\sum_i M_i^{n,k+1/2}\psi_i^{up\ n,k+1/2} - (\beta_2^+\psi^{n+1,k+1} + \beta_2^-\psi^{n,k+1})\sum_i M_i^{n,k+1/2}\right] \\
&\left.-\rho^{n,k-1/2}\left[\sum_i M_i^{n,k-1/2}\psi_i^{up\ n,k-1/2} - (\beta_2^+\psi^{n+1,k} + \beta_2^-\psi^{n,k})\sum_i M_i^{n,k-1/2}\right]\right\}
\end{aligned}
$$

with $\beta_1^+ = 1 - \beta_1^-$ and $\beta_2^+ = 1 - \beta_2^-$ the implicit weights. A fully implicit solver, i.e., $\beta_1^+ = \beta_2^+ = 1$, is mostly used here. A tridiagonal matrix solver is used to solve $\mathbf{A}\cdot\Psi^{n+1} = \mathbf{d}$ for Ψ^{n+1}.
For $2 \le k \le N_k - 1$ the coefficients are given as

$$
\begin{aligned}
a_k &= \frac{\rho^{n,k-1/2}}{\rho^{n,k}\Delta z^k}\left[\beta_1^+\frac{K^{n,k-1/2}}{\Delta z^{k-1/2}}\right] \\
b_k &= -\frac{1}{\Delta t} + \frac{\rho^{n,k+1/2}}{\rho^{n,k}\Delta z^k}\left[-\beta_1^+\frac{K^{n,k+1/2}}{\Delta z^{k+1/2}}\right] - \frac{\rho^{n,k-1/2}}{\rho^{n,k}\Delta z^k}\left[\beta_1^+\frac{K^{n,k-1/2}}{\Delta z^{k-1/2}} + \beta_2^+\sum_i M_i^{n,k-1/2}\right] \\
c_k &= \frac{\rho^{n,k+1/2}}{\rho^{n,k}\Delta z^k}\left[\beta_1^+\frac{K^{n,k+1/2}}{\Delta z^{k+1/2}} + \beta_2^+\sum_i M_i^{n,k+1/2}\right] \\
d_k &= -\frac{\psi^{n,k}}{\Delta t} - \frac{1}{\rho^{n,k}\Delta z^k}\left\{\frac{K^{n,k+1/2}\rho^{n,k+1/2}}{\Delta z^{k+1/2}}\beta_1^-\left[\psi^{n,k+1} - \psi^{n,k}\right] - \frac{K^{n,k-1/2}\rho^{n,k-1/2}}{\Delta z^{k-1/2}}\beta_1^-\left[\psi^{n,k} - \psi^{n,k-1}\right]\right. \\
&\quad+\rho^{n,k-1/2}\left[\sum_i M_i^{n,k-1/2}\psi_i^{up\ n,k-1/2} - \beta_2^-\psi^{n,k}\sum_i M_i^{n,k-1/2}\right] \\
&\quad\left.-\rho^{n,k+1/2}\left[\sum_i M_i^{n,k+1/2}\psi_i^{up\ n,k+1/2} - \beta_2^-\psi^{n,k+1}\sum_i M_i^{n,k+1/2}\right]\right\}.
\end{aligned}
$$

The boundary conditions at the surface are specified for $k = 1$, as

$$
\begin{aligned}
a_k &= 0\\
b_k &= -\frac{1}{\Delta t} + \frac{\rho^{n,k+1/2}}{\rho^{n,k}\Delta z^k}\left[-\beta_1^+ \frac{K^{n,k+1/2}}{\Delta z^{k+1/2}}\right] - \beta_1^+ |\mathbf{v_{h1}}| C_\psi^n/\Delta z^k\\
c_k &= \text{same as for } 2 \le k \le N_k - 1\\
d_k &= -\frac{\psi^{n,k}}{\Delta t} - \frac{1}{\rho^{n,k}\Delta z^k}\left\{\frac{K^{n,k+1/2}\rho^{n,k+1/2}}{\Delta z^{k+1/2}}\beta_1^-\left[\psi^{n,k+1} - \psi^{n,k}\right]\right.\\
&\left. -\rho^{n,k+1/2}\left[\sum_i M_i^{n,k+1/2}\psi_i^{up\ n,k+1/2} - \beta_2^-\psi^{n,k+1}\sum_i M_i^{n,k+1/2}\right]\right\} + |\mathbf{v_{h1}}|\frac{C_\psi^n}{\Delta z^k}\left[\beta^-\psi^{n,k} - \psi_s\right]
\end{aligned}
$$

This formulation with Dirichlet boundary conditions makes use of the drag coefficients computed in the surface scheme and through (**??**). The user can, however, also decide to use a Neuman boundary condition (`doneuman=.true.`) using the fluxes from the surface scheme and from (**??**). In this case, the last rhs term in b_k is dropped and the last term in d_k becomes $-\overline{\psi' w'}^n/\Delta z^k$ makeing the surface fluxes fully explicit. This explicit Neuman boundary condition is also used if surface fluxes are prescribed (`sfc_tau_fxd` or `sfc_flx_fxd` respectively).

The boundary condition at the top for $k = N_k$ is given as

$$
\begin{aligned}
a_k &= \text{same as for } 2 \le k \le N_k - 1\\
b_k &= -\frac{1}{\Delta t} - \frac{\rho^{n,k-1/2}}{\rho^{n,k}\Delta z^k}\left[\beta_1^+ \frac{K^{n,k-1/2}}{\Delta z^{k-1/2}} + \beta_2^+ \sum_i M_i^{n,k-1/2}\right]\\
c_k &= 0\\
d_k &= -\frac{\psi^{n,k}}{\Delta t} + \frac{1}{\rho^{n,k}\Delta z^k}\left\{\frac{K^{n,k-1/2}\rho^{n,k-1/2}}{\Delta z^{k-1/2}}\beta_1^-\left[\psi^{n,k} - \psi^{n,k-1}\right]\right.\\
&\left. -\rho^{n,k-1/2}\left[\sum_i M_i^{n,k-1/2}\psi_i^{up\ n,k-1/2} - \beta_2^-\psi^{n,k}\sum_i M_i^{n,k-1/2}\right]\right\}.
\end{aligned}
$$

Again, ρ needs to be replaced by ρ_d in case of $\psi = r_v$ or $\psi = e$.

4.2 TKE equation

The numerical implementation to advance e from step n to step $n+1$ is as follows. SHEAR, BUOY, and DISS are treated explicitly with an Euler step. Thereby, K_m at step n is diagnosed from e at step n. This is for example different in SAM where K^n is obtained from an intermediate e. What's generally done here? Also is TRANS computed on the intermediate e or e at step n. The three tendencies will be limited in magnitude to ensure their sum is not smaller than $-\frac{e}{\Delta t}$. Then, TRANS is computed as described below (general formulation allowing for an implicit solver) again based on the e distribution (and K) at step n. That means that TRANS may still cause some negative e at step $n+1$ since the solver for TRANS is not necessarily positive definite. Negative e will be clipped at the beginning of the next step. The advective term ADV is eventually computed by the Dycore which has TKE per mass of moist air as prognostic variable such that conversion is required before passing over and receiving e (i.e., analogous to the water vapor mixing ratio).

The buoyancy flux at time n is needed in the buoyancy production term. The ED part of the flux requires knowledge about $K = C_k l e^{1/2}$. e is available from the previous timestep (if a diagnostic scheme would be used then e might still get advected by the Dycore and is thus treated like a prognostic variable) but l needs to be re-evaluated at step n. To this end, the boundary layer height h is required (since $l\ \tau e^{1/2}$ and $\tau\ h/w^*$). It is computed either consistently at step n if defined as the height where the θ_v gradient at step n is maximized or somewhat inconsistently if defined as the height where the buoyancy flux at $n-1$ gets minimized. Note that h is also required as input to the mupliplume model and the same strategy is applied there. The MF fluxes at step n might be included in the buoyancy flux of the buoyancy generation term (as done in the Witek scheme) and the plume model is thus called before evaluating the TKE sources.

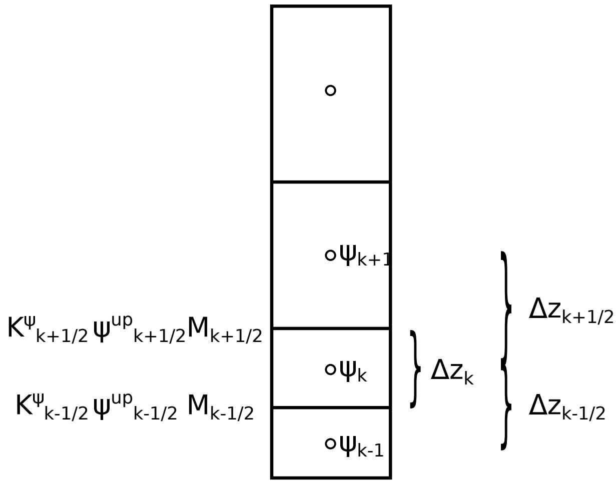

Figure 1: Locations of prognostic variable ψ, the updraft mass fluxes M_i, the updraft properties ψ_i^{up}, and eddy-diffusivities K^{ψ} on the 1D vertical grid.

5 Design strategy

SAM's prognostic variables are:

- $h_{il} = c_p T + gz - L_v(q_c + q_r) - L_s(q_i + q_s + q_g)$
- $q_t = q_v + q_n = q_v + q_c + q_i$
- u, v, w
- e

with q indicating a mixing ratio per mass of dry air and h_{il} the moist static energy conserved under mass-conserving phase changes including liquid and frozen water. The indices c, i, r, s, g represent non-precipitating cloud liquid water and cloud ice and precipitating rain, snow, and graupel. Note that a flux of h_{il} is related to a flux in θ_{il}, the liquid/frozen water potential temperature, as

$$\overline{w'\theta'_{il}} = \frac{1}{c_p}\frac{\theta}{T}\overline{w'h'_{il}} \tag{48}$$

with $\frac{\theta}{T} = (p_0/p)^{R_d/c_p}$.

The idea here is to implement a PBL and shallow cumulus scheme into SAM. The commonly used Deardorff TKE closure is then switched off. Therefore, no explicit horizontal diffusion will be computed in this new version and vertical mixing will be applied only in the boundary layer. The mixing outside of the boundary layer is thus handled truly implicitly by the diffusive advection scheme.

The outline of a timestep to go from step n (time t) to step $n+1$ (time $t+\Delta t$):

5.1 1) Get surface fluxes

Use existing scheme in SAM.

5.2 2) Run PDF condensation scheme

Given the mean prognostic variables for each grid cell we first run the PDF cloud scheme to retrieve the mean condensed water content $q_n = q_c + q_i$, an SGS cloud fraction, and the grid-scale buoyancy flux. The procedure follows closely the strategy outlined by Sommeria and Deardorff (1977), Bougeault (1981), and Bechtold et al. (1995) but is extended here to account for frozen water. In short, the PDF scheme requires as input the grid-scale mean values of $\theta_{il}^* = \theta - \frac{\theta}{T}(L_v/c_p q_c + L_s/c_p q_i)$ and $q_t = q_v + q_c + q_i$ and the standard deviation σ_s of the saturation deficit.

We derive σ_s from vertical gradients in θ_{il}^* and q_t following Bechtold et al. (1995). Same as in Cheinet and Teixeira (2003), we assume a constant length scale in the formulation of σ_s (this will allow for a explicit formulation since the master length scale from the TKE scheme is unknown at this point). The condensation scheme is called only in the presence of turbulent kinetic energy.

Since only q_t is known a priori, an iterative approach is used here to derive the potential temperature needed in θ^*_{il}. We use the same strategy that is applied in the all-or-nothing adjusment scheme that is called at the end of a time step in SAM (as long as SAM's default single moment microphysics scheme is used). Thereby, a first guess for θ^*_{il} is made by assuming no condensate at all such that $h^*_{il} = h_{il}$. This gives a first guess on temperature T which is then used to partition q_p into q_r, q_s, and q_g following the descriptions given by Khairoutdinov and Randall (2003). A second guess for h^*_{il} is then possible by updating $h^*_{il} = h^*_{il} + L_v q_r + L_s(q_s + q_g)$. This yields a first guess for θ^*_{il}.

Then, the iterative procedure starts by computing the vertical gradient of θ^*_{il} to get σ_s as input to the PDF condensation scheme. The latter returns the cloud condensate q_n which can be partitioned by temperature into q_c and q_i following Khairoutdinov and Randall (2003). Given the partitioned cloud condensate the iteration loop ends by evaluating a new θ^*_{il} from θ_{il}.

This scheme will thus add an additional source for latent heat release based on SGS clouds to SAM. We keep the grid-scale all-or-nothing scheme at the end of the time step. As described in Sommeria and Deardorff (1977), we expect that the onset of cloud formation in the boundary layer is simulated less abruptly with this formulation since clouds form before saturation at the grid-scale occurs. More importantly, this way we account for unresolved condensation as found in stratocumulus layers.

Note that we assumed in this procedure that the mean grid-scale values of the prognostic variables equal their environmental values outside of plumes. The stratiform cloud cover is usually thought to affect the environment around plumes only. This is ignored here.

5.3 3) Evaluate mixing length and eddy diffusivities

Thanks to the PDF scheme, we have the mean grid-scale potential temperature θ_v (which was unknown before the adjustment). Given θ_v and turbulent kinetic energy e we can evaluate the stability dependent turbulent length scale l. In turn, we can derive the eddy diffusivities K.

5.4 4) Run plume model

Given the mean grid-scale potential temperature θ_v, we can now solve the plume equations

$$\frac{d\psi_i^{up}}{dz} = -\epsilon(\psi_i^{up} - \psi) \qquad (49)$$

with entrainment rate ϵ and the environmental value ψ. The parcel rises until its vertical velocity reaches zero. The latter is given by Simpson and Wiggert (1969)'s parameterization

$$1/2\frac{d(w_i^{up})^2}{dz} = aB_i^{up} - (b + c\epsilon)(w_i^{up})^2 \qquad (50)$$

with ψ_i either θ_{il} or total water $q_t + q_p$ for plume i. Note that we assume that the plume environment is well represented by the grid-mean values and that the buoyancy is given as the potential temperature difference to the grid-scale mean (which we know from the previous adjustment).

This yields the MF part of the vertical fluxes of the prognostic variables.

5.5 5) Advection

SAM's advection of scalars and momentum. Solve for Poisson pressure.

5.6 6) Implicit solve for mixing tendencies

Given the eddy diffusivities and the mass fluxes we can advance the prognostic variables due to mixing.

5.7 5) Grid-scale microphysics and all-or-nothing adjustment

The simple 1-moment scheme described in Khairoutdinov and Randall (2003) is used. It envokes the already mentioned adjustment scheme but in a all-or-nothing approach. Both cloud condensate and precipitating condensate are partitioned into subcategories based on temperature. Then, microphysical conversion rates are evaluated to update q_n and q_p. A mean fall velocity is evaluated which is used for sedimentation (which is computed in section 5). Update the cloud fraction to one if saturated on the grid-scale.

5.8 6) Radiation

Use the liquid water and ice water path. Both now include contributions from the PDF scheme. Similary, the cloud fraction in the grid box might be larger than zero even if the grid-box is unsaturated on average. If saturated on average, then the cloud fraction in the box is one.

References

Bechtold, P., J. W. M. Cuijpers, P. Mascart, and P. Trouilhet, 1995: Modeling of trade wind cumuli with a low-order turbulence model: Toward a unified description of cu and se clouds in meteorological models. *Journal of the Atmospheric Sciences*, **52 (4)**, 455–463.

Bougeault, P., 1981: Modeling the trade-wind cumulus boundary layer. part I: Testing the ensemble cloud relations against numerical data. *Journal of the Atmospheric Sciences*, **38 (11)**, 2414–2428.

Bryan, G. H., J. C. Wyngaard, and J. M. Fritsch, 2003: Resolution requirements for simulations of deep moist convection. *Mon. Wea. Rev.*, **131**, 2394–2416.

Cheinet, S., 2003: A multiple mass-flux parameterization for the surface-generated convection. Part I: Dry plumes. *J. Atmos. Sci.*, **60**, 2313–2327.

Cheinet, S. and J. Teixeira, 2003: A simple formulation for the eddy-diffusivity parameterization of cloud-topped boundary layers. *Geophys. Res. Lett.*, **30**, 1930.

Collins, W. D., P. J. Rasch, B. A. Boville, J. J. Hack, J. R. McCaa, D. L. Williamson, J. T. Kiehl, and B. Briegleb, 2004: Description of the NCARG Community Atmosphere Model (CAM 3.0). NCAR Technical note TN464+STR, National Center for Atmospheric Research, USA.

Han, J., 2015: Implementation in the NCEP GFS of a hybrid eddy-diffusivity mass-flux (EDMF) boundary layer parameterization with dissipative heating and modified stable boundary layer mixing. *Wea. Forecasting*, submitted.

Khairoutdinov, M. F. and D. A. Randall, 2003: Cloud resolving modeling of the ARM summer 1997 IOP: Model formulation, results, uncertainties, and sensitivities. *J. Atmos. Sci.*, **60**, 607–625.

Lenschow, D. H., J. C. Wyngaard, and W. T. Pennell, 1980: Mean-field and second-moment budgets in a baroclinic, convective boundary layer. *J. Atmos. Sci.*, **37**, 1313–1326.

Neggers, R. A. J., A. P. Siebesma, and H. J. J. Jonker, 2002: A multiparcel model for shallow cumulus convection. *J. Atmos. Sci.*, **59**, 1655–1668.

Simpson, J. and V. Wiggert, 1969: Models of precipitating cumulus towers. *Mon. Wea. Rev.*, **97**, 471–489.

Soares, P. M. M., P. M. A. Miranda, A. P. Siebesma, and J. Teixeira, 2004: An eddy-diffusivity/mass-flux parametrization for dry and shallow cumulus convection. *Quart. J. Roy. Met. Soc.*, **130 (604)**, 3365–3383.

Sommeria, G. and J. W. Deardorff, 1977: Subgrid-scale clouds in models of nonprecipitating clouds. *J. Atmos. Sci.*, **34**, 344–355.

Sorbjan, Z., 1991: Evaluation of local similarity functions in the convective boundary layer. *Journal of Applied Meteorology*, **30 (12)**, 1565–1583.

Sušelj, K., T. F. Hogan, and J. Teixeira, 2014: Implementation of a stochastic eddy-diffusivity/mass-flux parameterization into the Navy Global Environmental Model. *Wea. Forecasting*, **29**, 1374–1390.

Sušelj, K., J. Teixeira, and D. Chung, 2013: A unified model for moist convective boundary layers based on stochastic eddy-diffusivity/mass-flux parameterization. *J. Atmos. Sci.*, **70**, 1929–1953.

Sušelj, K., J. Teixeira, and G. Matheou, 2012: Eddy diffusivity/mass flux and shallow cumulus boundary layer: An updraft pdf multiple mass flux scheme. *J. Atmos. Sci.*, **69**, 1513–1533.

Teixeira, J. and S. Cheinet, 2004: A simple mixing length formulation for the eddy-diffusivity parameterization of dry convection. *Bound.-Lay. Meteor.*, **110 (3)**, 435–453.

Tiedtke, M., 1989: A comprehensive mass flux scheme for cumulus parameterization in large-scale models. *Mon. Wea. Rev.*, **117**, 1779–1800.

Witek, M. L., J. Teixeira, and G. Matheou, 2011: An integrated TKE-based eddy diffusivity/mass flux boundary layer closure for the dry convective boundary layer. *J. Atmos. Sci.*, **68**, 1526–1540.